

LA-UR-14-22884

Approved for public release; distribution is unlimited.

Title: Effect of Mach number on Richtmyer-Meshkov mixing and transition

Author(s):
Orlicz, Gregory C.
Balasubramanian, Sridhar
Prestridge, Katherine P.

Intended for: Conference proceedings paper for Nuclear Engineering Design Physics Conference (NEDPC) March 2014

Issued: 2014-04-25



Disclaimer:

Los Alamos National Laboratory, an affirmative action/equal opportunity employer, is operated by the Los Alamos National Security, LLC for the National Nuclear Security Administration of the U.S. Department of Energy under contract DE-AC52-06NA25396. By approving this article, the publisher recognizes that the U.S. Government retains nonexclusive, royalty-free license to publish or reproduce the published form of this contribution, or to allow others to do so, for U.S. Government purposes.

Los Alamos National Laboratory requests that the publisher identify this article as work performed under the auspices of the U.S. Department of Energy. Los Alamos National Laboratory strongly supports academic freedom and a researcher's right to publish; as an institution, however, the Laboratory does not endorse the viewpoint of a publication or guarantee its technical correctness.

(U) Effect of Mach number on Richtmyer-Meshkov mixing and transition

Greg Orlicz, Sridhar Balasubramanian, and Kathy Prestridge

Los Alamos National Laboratory, Los Alamos, NM

(Unclassified) In the current work we focus on the mixing transition to smaller scales that occurs as a result of the growing Richtmyer-Meshkov (R-M) instability for 3 different Mach number cases ($M = 1.21, 1.36, \text{ and } 1.50$). The high temporal resolution of the velocity and density measurements allows for the most complete picture of the R-M mixing transition to date. Several metrics are presented to assess the state of the mixing layer throughout time. It is found that increasing the Mach number has the effect of decreasing the amount of mixing (in the sense of how much molecular mixing has taken place), but increasing the homogeneity across the mixing layer at a given scaled time. Estimates of turbulent kinetic energy (TKE) are found using both an instantaneous, spatially-averaged basis, and an ensemble-averaged basis. Results suggest that spatially averaging over instantaneous realizations is inappropriate for estimating TKE at earlier times, but appears to be a reasonable estimate at later times. Several other metrics are presented, including the evolution of the density-specific-volume correlation parameter, b , from the BHR model.

Introduction

The Richtmyer-Meshkov (R-M) instability is an important process that governs fluid mixing in engineering applications where shock waves are present. As the instability grows in time, the flow may eventually transition to a turbulent state with a broad range of relevant length scales and complicated flow features on a very short time scale, making it a challenging problem to investigate both experimentally and numerically. Experiments are performed to study the effect of incident shock Mach number (M) on the development of the R-M instability after a shock wave impulsively accelerates a varicose-perturbed, heavy-gas curtain (air-SF₆-air). The resulting instability and subsequent fluid mixing is measured using simultaneous Planar Laser-Induced Fluorescence (PLIF) and Particle Image Velocimetry (PIV). The implementation of both of these diagnostics is particularly important for the study of variable density flows in which the scalar mixing state actively modulates the flow dynamics. Turbulence in variable density flows is therefore more complicated, and our understanding is limited compared to more classical turbulence problems.

Experimental Facility

The experiments were performed at the Los Alamos horizontal gas shock tube. A schematic of the facility is shown in Fig. 1. A detailed description of its operation can be found in the literature.¹ The

initial conditions consist of a thin, varicose perturbed, heavy gas curtain surrounded by air. The heavy gas is a mixture of sulfur hexafluoride (SF₆), air, acetone, and glycol droplets. The heavy gas mixture is allowed to flow by gravity through a special nozzle with an exit aligned with the top wall of the shock tube. The resulting row of closely spaced jets that flow through the test section make up the gas curtain initial conditions with a perturbation wavelength of 3.6 mm. At the primary x - y measurement plane located 2 cm below the top wall of the shock tube, the peak SF₆ volume fraction along the center line of the curtain is estimated to be $\sim 45\%$, with 12% acetone vapor and 43% air by volume. The Atwood number for this mixture composition is $A = 0.49$.

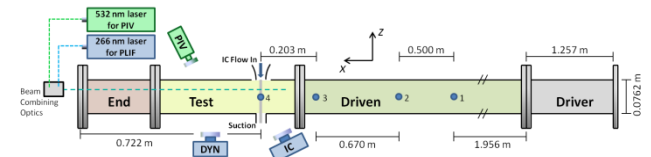


Fig. 1. Schematic of experimental facility.

Density and velocity measurements were obtained using two dual headed pulsed lasers with output frequencies of 266 nm for PLIF, and 532 nm for PIV. The lasers are co-aligned and formed into sheets, with the 266 nm frequency causing the acetone tracer to fluoresce, while the 532 nm is scattered off of the fog droplets.

Results

A selection of PLIF based density maps showing the evolution of the gas curtain with time are presented in Fig. 2. Images along a row show the mixing layer at the same streamwise distance from the initial condition location for each Mach number, and can be thought of as scaled time in this study. The contrast for each image in Fig. 2 has been adjusted to highlight the flow features.

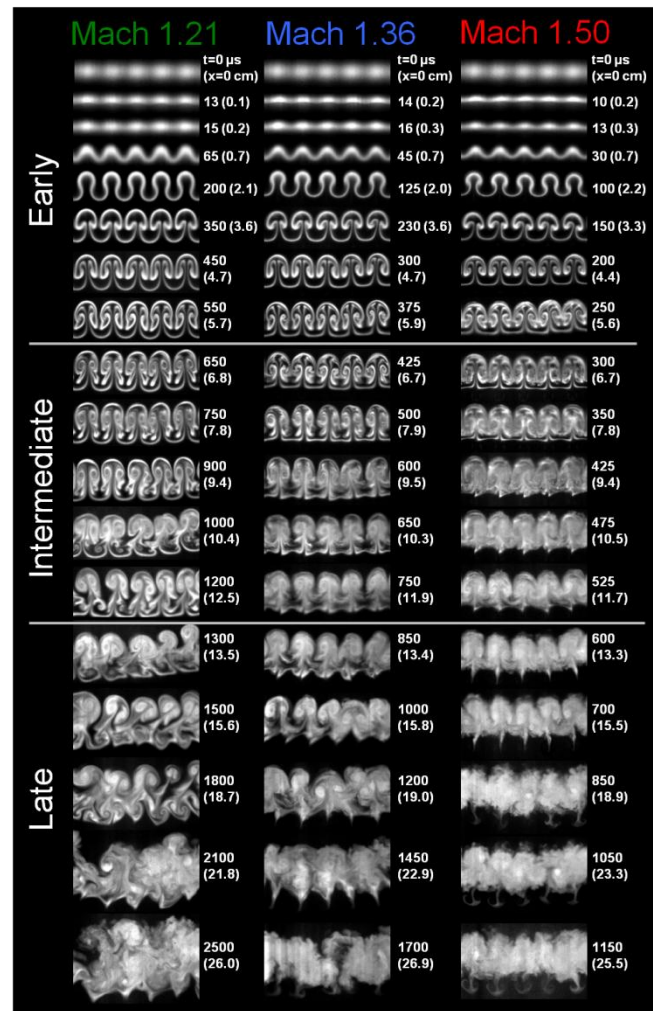


Fig. 2. A selection of density maps from each Mach number experiment. Images in each row were acquired at roughly the same location as indicated in the figure, with time t and distance traveled (x).

At early times, up to $x \sim 6$ cm, the evolution of the curtain appears similar for each Mach number. Throughout intermediate times, from 6 cm to 13 cm, the structures begin to grow differently. At late times, $x > 13$ cm, the structures become increasingly disordered with more apparent small scale mixing, and the differences observed at intermediate times become more enhanced. By the latest times visualized, regions within the mixing layer resemble turbulence for each Mach number.

Amount of Mixing Quantified

Using the scaled time, x , appears to be an effective way to collapse many of the quantities investigated in this study, including the total mixing width, shown in Fig. 3. Here a scaled width, $\delta^* = \frac{\delta}{\delta_0} M^{-0.4}$, is used

on the vertical axis, where δ_0 is the just shocked and compressed mix width for each case. Mix width shows the spatial extent to which light and heavy gases have interpenetrated. While mix width is a common metric used to compare amongst experiments and simulations, it tells us only about the largest scale in the flow, and nothing about how much molecular mixing has actually occurred between the two gases.

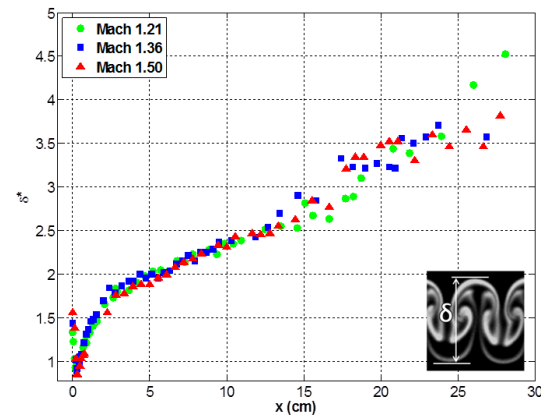


Fig. 3. Scaled mix width as a function of downstream location, x , also referred to as scaled time.

One way to quantify the amount of molecular mixing in this flow is to consider the average volume fraction of the SF₆, \bar{c}_v . As the flow evolves, and molecular mixing occurs, the heavy gas will become

more and more diluted by the surrounding air, and hence \bar{c}_v will decrease. Fig. 4 shows the evolution of \bar{c}_v with downstream location. We find lower values for lower Mach numbers, indicating that lower Mach numbers actually produce more molecular mixing by the time the mixing layer arrives at a given downstream location.

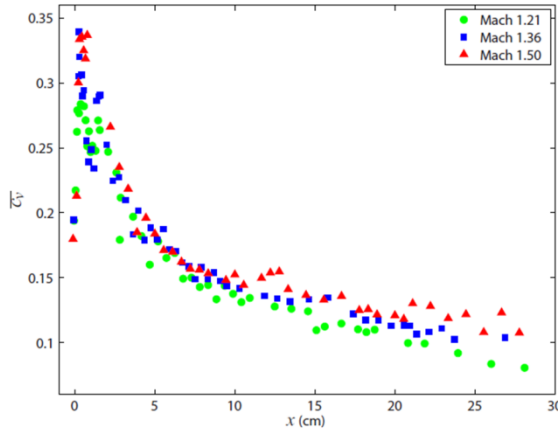


Fig. 4. \bar{c}_v as a function of distance traveled.

It is important to note the distinction between the amount of molecular mixing – a measure of how diluted the heavy gas has become with air, and the uniformity of the mixing. As can be seen in Fig. 2, higher Mach numbers appear to produce more homogeneous structures at late times.

This can also be seen in PDFs of the density field shown in Fig. 5. As time progresses from early to late times, the peak distribution for all Mach numbers becomes increasingly narrow, indicating increasing mixing uniformity for all cases, with peak probabilities at higher concentrations for higher Mach numbers, indicating that as M increases, less pure air is molecularly mixed with the heavy gas. A double peak is observed in some of the PDFs for Mach 1.21 experiments at late times. This structure reflects the large amount of low density gas that penetrates well into the mixing layer in low Mach number experiments. In Mach 1.50 experiments, the uniformity of the mixing layer is much higher, and this is quantified by the much narrower peak in the PDFs at $0.1 < \bar{c}_v < 0.2$.

Another measure of mixing progress, Ξ , can be obtained through mixture composition fields, first

applied by Cook and Dimotakis² to Rayleigh-Taylor flows. For more details on how Ξ is calculated in the current study, see Orlicz *et al.*¹ Ξ indicates how much mixing has occurred relative to how much mixing could occur if all entrained fluid were completely mixed at each streamwise location, and varies from 0 (if two fluids are spatially segregated) to 1 (if two fluids are uniformly mixed at each streamwise location). Therefore, Ξ is a measure of mixing uniformity.

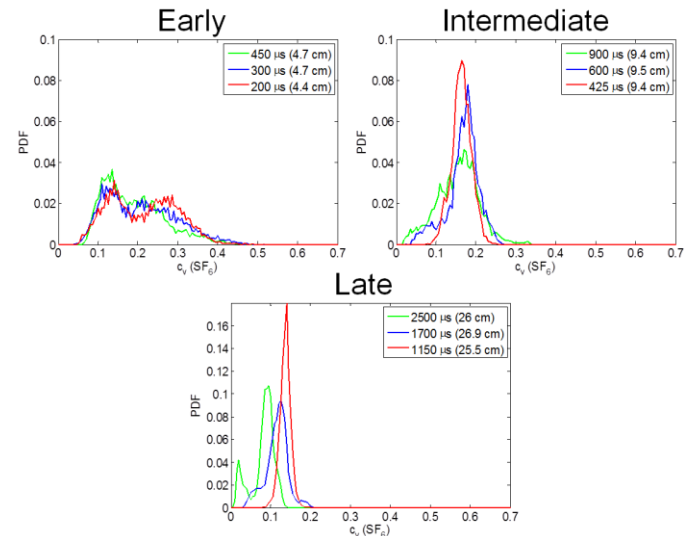


Fig. 5. PDFs for volume fraction of SF₆ for each Mach number at 3 different scaled time regimes. green – M=1.21; blue – M=1.36; red – M=1.50.

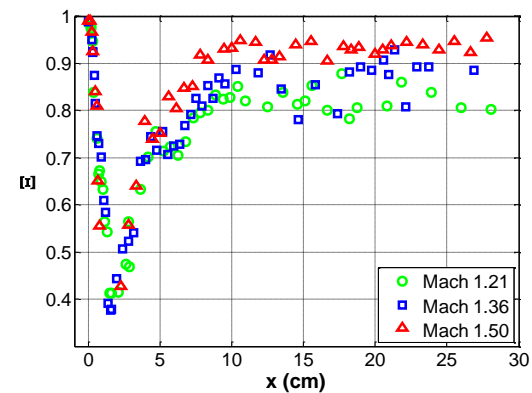


Fig. 6. Evolution of Ξ with distance traveled.

In Fig. 6, Ξ is shown vs. distance traveled. Initially, Ξ is high for all cases, as the diffuse initial

conditions are relatively uniform in the spanwise direction. As the deposited vorticity causes the instability to grow, air is entrained in the mixing layer, and thus Ξ decreases rapidly, reaching a low at $x \sim 2$ cm for each Mach number case. Small scale stirring mechanisms then begin contributing to mixing uniformity and Ξ begins increasing rapidly for each Mach number. After $x = 10$ cm, Ξ appears to asymptote for each case, with higher values reflecting the increased mixing homogeneity for higher Mach numbers.

To provide insight into these differences in mixing when Mach number is varied, we consider the total instantaneous mixing rate, χ_{total} , shown as a function of real time in Fig. 7. $\chi(x,y)$ provides a measure of how quickly molecular mixing is occurring throughout the flow, and where it is occurring spatially. Therefore, it can be used to understand the processes that are driving the mixing between the two fluids, and what differences may exist between the different Mach number cases. More details on the calculation of χ_{total} can be found in the literature.^{1,3}

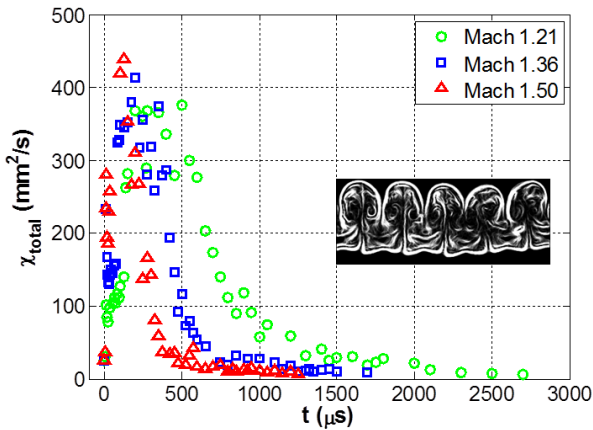


Fig. 6. Evolution of χ_{total} with time.

In Fig. 7, χ_{total} is shown as a function of time, t . Each data point represents the spatial integration over x and y of the 2D $\chi(x,y)$ map. Therefore, it gives the instantaneous mixing rate of each structure. An indication of how much mixing has taken place can be obtained if χ_{total} is integrated over real time. It is apparent from Fig. 7 that much higher values are obtained for lower Mach number if χ_{total} is integrated

over time, and therefore, one can infer more molecular mixing for lower Mach number experiments.

The observation that lower Mach number shock waves generate more mixing at the same scaled time appears to be due to the additional absolute time and the additional interfacial length (see Orlicz et al.¹) over which diffusion-driven molecular mixing acts. The interface length is a direct consequence of the dynamics of the vortex interaction, with stronger vortices limiting the amount of pure air that can penetrate into the mixing layer. Vorticity production is an important mechanism that determines the mixing state at later times by establishing the larger scale features. In addition to driving the energy transfer to smaller length scale advective stirring, the large scale features also drive the molecular mixing through diffusion. In higher Mach number experiments, the degree of advective stirring is higher, but this ultimately limits the amount of molecular mixing that can take place on average throughout the mixing layer.

Measures of Turbulence

The current data provide a unique opportunity to investigate the evolution of turbulence related quantities in an R-M transitioning flow with high temporal resolution. Consequently, these results may prove useful for current modeling and validation efforts. Below we present some relevant measures of turbulence.

Velocity fluctuations

Probability density functions (PDFs) for the fluctuations of both components of velocity are presented in Fig. 7 at both early times (top row) and late times (bottom row). Velocity fluctuations, u' and v' were calculated as deviations from the whole field mean of an instantaneous realization. Because turbulence is characterized by large intermittent fluctuations in velocity, the PDFs in a developing turbulent flow tend to develop non-Gaussian profiles with long tails. Such profiles are observed at earlier times for the streamwise component, u' , for all three Mach numbers, but caution is required in the interpretation of these PDFs because they are calculated from single realizations. As a result, this

feature is not necessarily an indication of a turbulent flow field in these experiments. Meanwhile, the PDFs of the spanwise component, v' , have relatively short tails. The PDFs of v' also tend to be symmetric about the mean, owing to the spanwise symmetry of the flow. However, at earlier times the PDFs of u' tend to be asymmetric with a higher probability for extreme negative (upstream) fluctuations than for extreme positive fluctuations. This is presumably due to the directionality of the shock wave. As time progresses, both distributions become increasingly narrow about the 0 value, and the PDFs for u' become more symmetric with much shorter tails, indicating that if the flow can be defined as turbulent, the turbulence is decaying. That the profiles of both the u' and v' PDFs are similar at late times also indicates the flow is tending toward isotropy and losing memory of the initial conditions. Comparing between Mach numbers, the PDFs of both u' and v' are wider with increasing M for a given scaled time, x , indicating a wider range of scales over which velocity fluctuations occur, as more energy is deposited by higher Mach number shock waves.

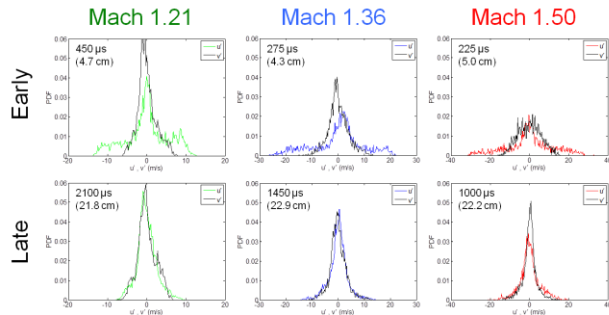


Fig. 7. PDFs of velocity fluctuations, u' (color) and v' (black) at two different scaled time regimes.

Evolution of turbulent kinetic energy estimates

From the velocity fluctuations, we estimate the turbulent kinetic energy (TKE) field from available components as

$$K_{12}(x, y) = \frac{1}{2}(u'^2(x, y) + v'^2(x, y)), \quad (1)$$

where the subscript, '12', indicates that TKE estimates were calculated from the streamwise and spanwise components of velocity only (and not the

vertical out of plane component). The use of instantaneous realizations to estimate TKE, while not strictly correct, is still valuable for validation of numerical simulations where averages must also be obtained from single realizations. In many RMI experiments, it is also not practical to acquire enough data for statistical convergence. In the current study, the spanwise repetitiveness of the flow lends itself to averaging over each wavelength, essentially providing five times the data to arrive at better estimates for TKE using ensemble averaging. In Fig. 8 the evolution of $\overline{K_{12}}(x, y)$ scaled by the mixing layer velocity jump squared, Δu^2 , is shown for each Mach number. Here, over bar indicates the spatial average value of $K_{12}(x, y)$. Values for $\overline{K_{12}}(x, y)$ using average velocities obtained from instantaneous spatial averaging are shown in color. Values for $\overline{K_{12}}(x, y)$ using average velocities obtained from ensemble averages of individual wavelengths are also shown in grey for times at which enough data was available to provide a better estimate of the true TKE. At earlier times, using an instantaneous basis over predicts TKE levels, but by scaled time $x = 13$ cm it appears to be a reasonable estimate. The point at which the two methods begin to agree, could be an indication of transition in the flow.

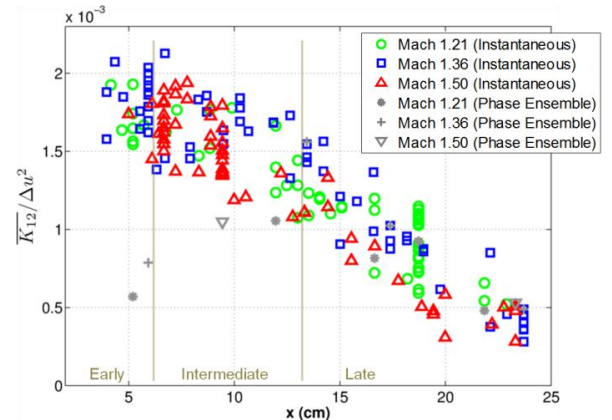


Fig. 8. TKE as a function of scaled time using two different bases for obtaining average velocities: spatially averaged instantaneous realizations (color), and ensemble averaged fields (grey).

Evolution of the density-specific-volume correlation parameter

The density-specific-volume correlation (b) appears as an unclosed multiplier in the production term of the mass flux equation for variable density flows and is an evolved quantity in the Los Alamos ‘BHR’ RANS turbulence model. The time evolution of the density-specific-volume correlation (b) can be derived from the density fields and can be used to determine how and when to turn on a subgrid turbulence model.

The density-specific-volume correlation can be defined using fluctuating or mean density fields as,

$$b = -\rho' \left(\frac{1}{\rho} \right)' = \bar{\rho} \left(\frac{1}{\rho} \right) - 1, \quad (2)$$

where ρ is the fluid density. By definition, b is non-negative and is equal to 0 when two fluids are homogeneously mixed. Conversely, high values of b indicate that the fluid is spatially inhomogeneous. In our curtain geometry, material projectiles that occur on the edges of the mixing layer can make large contributions to fluctuating quantities, biasing b to higher values. To limit the effect of these features, only the streamwise middle 20% region of the curtain was considered for calculations of b . Over this region,

$$b = \overline{\rho(x, y)} \left(\frac{1}{\rho} \right) (x, y) - 1, \quad (3)$$

where spatial averages have been taken over both x and y . Averaging b over all realizations at each time then gives $\langle b \rangle$. The evolution of $\langle b \rangle$ is presented in Fig. 9.

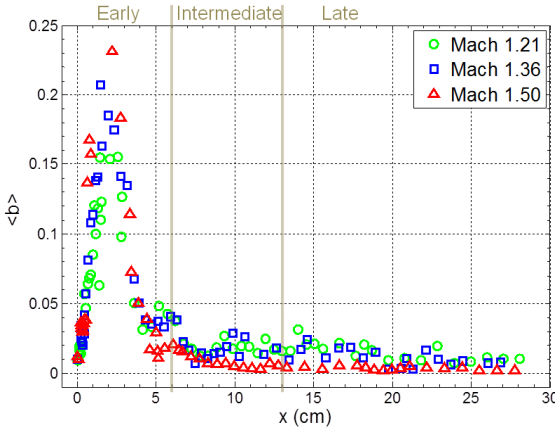


Fig. 9. $\langle b \rangle$ as a function of scaled time.

The value of $\langle b \rangle$ is initially low because the middle 20% of the layer contains only heavy gas. After shock interaction, the perturbations on the interface grow, and a peak in $\langle b \rangle$ occurs before the vortex cores are formed. As the vortex cores cause the mixing layer to roll up, $\langle b \rangle$ decays until smaller scale mixing is observed in the cores. Thereafter, $\langle b \rangle$ decreases much more slowly, and asymptotic behavior is observed.

In the region of $4.5 < x < 6.5$ we also observe a plateau feature for each Mach number in Fig. 9. It is during this time that the onset of small scale mixing in the vortex cores is observed, so this plateau feature serves as a quantitative marker for this transition. That this transition occurs at a similar scaled time, independent of Mach number, is a pattern that could be used to aid turbulence modeling, and is a potential candidate for when to turn on a turbulence model and what value to initialize it with.

Reynolds number

Using velocity measurements, it is possible to define the Reynolds number (Re) based on the average circulation, Γ of the main vortices or based on $\overline{K_{12}(x, y)}$ as follows:

$$Re_\Gamma = \frac{\Gamma}{v}, \quad Re_K = \frac{\sqrt{K_{12}}\delta}{v} \quad (4)$$

The kinematic viscosity, v was calculated using an average mixture composition across the mixing layer at post-shock conditions and was found to be $v = 8.2 \times 10^{-6}$, 7.1×10^{-6} , and $6.3 \times 10^{-6} \text{ m}^2/\text{s}$ for $M = 1.21$, 1.36 , and 1.50 , respectively. The evolution of Re with time based on both definitions is presented in Fig. 10. When the flow is dominated by the counter rotating vortex pairs, and the circulation based Re is more appropriate ($x < 13 \text{ cm}$), $Re_\Gamma \approx 8000$, 13000 , and 18000 for $M = 1.21$, 1.36 , and 1.50 , respectively. When the flow appears to be more turbulent and the TKE based Re number is more valid ($x \geq 13 \text{ cm}$), $Re_K \approx 3000$, 5000 , and 7000 . The currently accepted minimum value for fully developed turbulence to occur is $10,000$.³ Based on circulation, only Mach 1.36 and Mach 1.50 experiments meet this requirement.

Conclusions

We have found differences in both large- and small-scale mixing within a range of $1.2 \leq M \leq 1.5$ for fixed initial conditions by examining density and velocity fields in the temporally-evolving Richtmyer-Meshkov instability. Scaling the time axis with the velocity jump (convection velocity in the present case) of the mixing layer is sufficient to collapse mixing width data. The effectiveness of this scaling extends beyond the collapse of mix width growth rate data. For example, peaks in the evolution of b and χ_{total} , the plateau feature in b and minima in \mathcal{E} occur at the same downstream location for each Mach number.

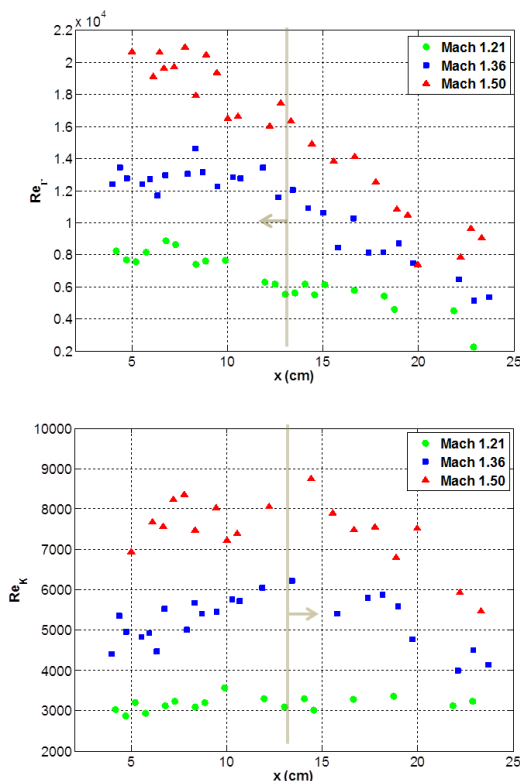


Fig. 10. Re as a function of scaled time using a circulation based definition (top), and a TKE based definition (bottom).

The quantities presented in this study provide information about how quickly mixing occurs, and how well mixed the two fluids become, both in terms

of the uniformity of mixing throughout the layer, and the degree to which air and heavy gas molecularly mix. Even when compared at the same downstream location, measurements show that higher incident Mach numbers lead to a more uniform mixing state. But lower incident Mach number yields greater mixing at a given downstream location if 'mixing' refers to entrainment or interpenetration of one fluid into another (mixing layer width), or to the amount of originally unmixed fluid that undergoes some molecular mixing (determined directly by mean volume fraction).

These results are also explained via differing vortex dynamics measured in each Mach number case using PIV. In higher Mach numbers, the vortices are stronger, entrain more heavy gas, and grow larger. While more proficient at advective stirring and the reduction of concentration gradients that exist in their vicinity, the vortices in the higher Mach number experiments also serve to limit the amount of pure air available for continued molecular mixing throughout the layer. Therefore, the mixing layers in higher Mach number experiments are more uniformly mixed, but on average across the mixing layer they are not as diluted by air as lower Mach number experiments.

While these results provide new insight into mixing mechanisms and processes in shock-induced variable density flows, this work may also be particularly useful as a validation and calibration tool for turbulent mixing models and numerical simulations. To this end, unprecedented measurements for an R-M flow showing the temporal evolution of turbulence related quantities, such as TKE and b , are given.

References

1. G. Orlicz *et al.*, "Incident shock Mach number effects on Richtmyer-Meshkov mixing in a heavy gas layer," *Physics of Fluids* 25, 114101 (2013);
2. C. Weber *et al.*, "Turbulent mixing measurements in the Richtmyer-Meshkov instability," *Physics of Fluids* 24, 074105 (2012).
3. P. Dimotakis, "The mixing transition in turbulent flows," *Journal of Fluid Mechanics* 409, pp. 69-98 (2000)